Sea Surface Currents in the Equatorial Pacific from VHF Radar Backscatter Observations

B. B. BALSLEY, A. C. RIDDLE,* W. L. ECKLUND AND D. A. CARTER

Aeronomy Laboratory, National Oceanic and Atmospheric Administration, Boulder, CO 80303

4 September 1986 and 7 January 1987

ABSTRACT

We present the analysis of three months of continuous sea-surface current data obtained by a VHF wind profiling radar at Christmas Island in the central equatorial Pacific. These results, which were obtained during the construction phase of the profiler when the antenna had not yet been phased to eliminate sea scatter, show a number of interesting features of the coastal flow, as well as the flow at greater distances from the island. We report here both the average surface current characteristics as well as features of the shorter-term variability. In addition, we discuss the idea that such sea-surface current measurements could be obtained quite easily in the central Pacific, provided that they were made in conjunction with existing and/or proposed profiler sites.

1. Introduction

In August 1985, NOAA's Aeronomy Laboratory began initial testing of a radar wind profiling system on Christmas Island (2°N, 157°W), Republic of Kiribati. The profiler will operate under the aegis of Project TOGA (Tropical Oceans Global Atmosphere) to transmit six-hourly winds aloft information via satellite to the Global Telecommunication Service (GTS) for dissemination to interested scientists. Higher time resolution data will be collected on magnetic tape for additional studies.

The purpose of the present note is not to report winds-aloft measurements, but rather to describe briefly a set of ocean backscatter observations that were obtained during a three-month testing period when the profiler operated in a mode that permitted a small amount of the total radio frequency energy to be radiated into three narrow antenna sidelobes directed horizontally over the nearby ocean. Analyses of the resulting sea-surface backscatter spectra that were obtained at ~140 second intervals throughout the test period comprise the observational content of this note.

We also discuss the idea that, based on our preliminary studies, routine sea surface currents could be obtained relatively easily in the equatorial Pacific by making use of the existing or proposed profiler sites, since most of the requisite equipment (e.g., laboratory building, power source, data recording system, etc.) is already in place.

2. Description of the system and Doppler sea-scatter spectra

The Christmas Island wind profiler is a 50 MHz pulsed Doppler radar operating with a peak transmitted power of about 40 kW and a pulse width of 8 microseconds (i.e., a range resolution of 1.2 km). Additional system details for a similar radar are given in Ecklund et al. (1979), and will not be repeated here.

Under normal operating conditions the antenna beam is switched sequentially through three high-elevation angle positions (one vertical position and two oblique positions toward the north and east, respectively, at zenith angles of 15°). Prior to final phasing adjustments of the antenna, however, a small portion (~0.2%) of the transmitted power was also radiated sequentially into the three narrow horizontal sidelobes (hereafter referred to as beams 1, 2 and 3) shown in Fig. 1.

Because of the strong backscatter cross section of the ocean surface relative to the backscatter cross section of the atmosphere, this small amount of horizontally transmitted power produced sea-scatter echoes that were typically much stronger than atmospheric echoes from the main antenna beam at comparable ranges. An example of the resulting Doppler spectrum obtained at a range of 5.5 km is shown in Fig. 2, where the strong bimodal peaks arising from the sea scatter via sidelobe 1 have been shaded to distinguish them from the normal atmospheric echo spectrum obtained on the vertical beam.

The general spectral characteristics of sea surface backscatter have been investigated in some detail (e.g., Barrick, 1972, Barrick et al., 1974; Lipa and Barrick, 1982, 1986). Indeed, the specific use of VHF wind profilers for sea-surface current monitoring has been investigated by Broche et al. (1987). These studies show that the scatter derives from sea-surface gravity waves traveling radially, i.e., along the antenna beam direction. The first order features of the sea-echo spectrum, as indicated in Fig. 2, consist of two narrow spectral peaks separated by twice the wave phase velocity V_ϕ, where V_ϕ for deep water conditions is given (Barrick, 1972) by

* Present affiliation: CIRES, University of Colorado, Boulder, CO 80309.

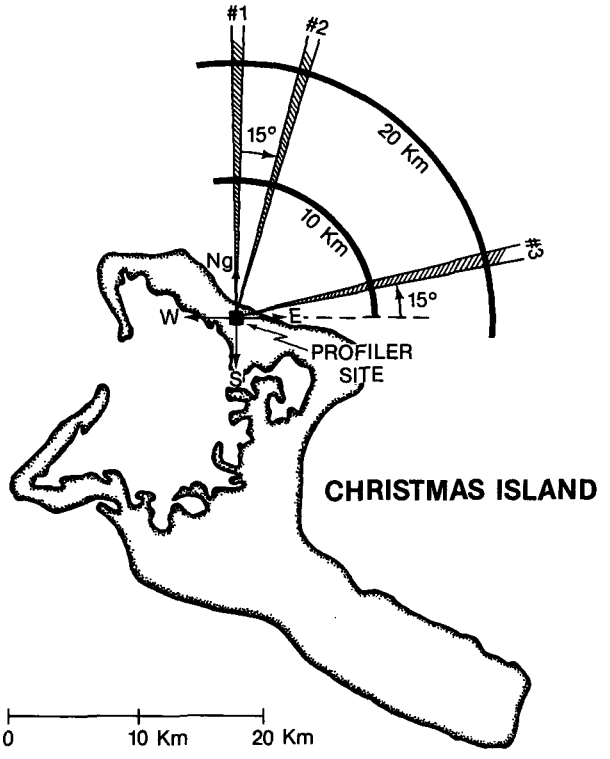

FIG. 1. Plan view of Christmas Island showing the profiler site and the three horizontal sidelobes that occurred during the installation phase, when the main antenna beam was directed respectively toward the vertical, east oblique, and north oblique positions.

$$V_\phi = \sqrt{gL/2\pi}.$$

Here L is the pertinent scale size (equal to one-half the radar wavelength λ) and g (= 9.81 m s^{-2}) is the acceleration due to gravity. For the present case the radar wavelength is 6.0 m, so that V_ϕ becomes 2.16 m s^{-1}, and the resulting peak separation is 4.32 m s^{-1}.

Both spectral peaks are Doppler shifted by the radial component of the ocean surface current along the beam direction. From a single antenna beam direction, it is possible to deduce the radial component of the total ocean surface current V_d along that beam by the relationship

$$V_d^k = \frac{V_+^k + V_-^k}{2}$$

where the positive and negative subscripted values refer to the velocities of the positive and negative peaks, and where the superscript refers to the specific beam direction (i.e., k = 1, 2 or 3). Figure 2 shows a positive 0.15 m s^{-1} displacement obtained from the northward directed horizontal slidelobe (beam 1 in Fig. 1), indicating a 0.15 m s^{-1} southward component of the surface current.

It is logical to extend the above single-beam capability to continuous radial measurements using two azimuthally separated beam directions, which enables continuous determination of the direction and the magnitude of the surface current vector, provided that the current can be assumed homogeneous within the

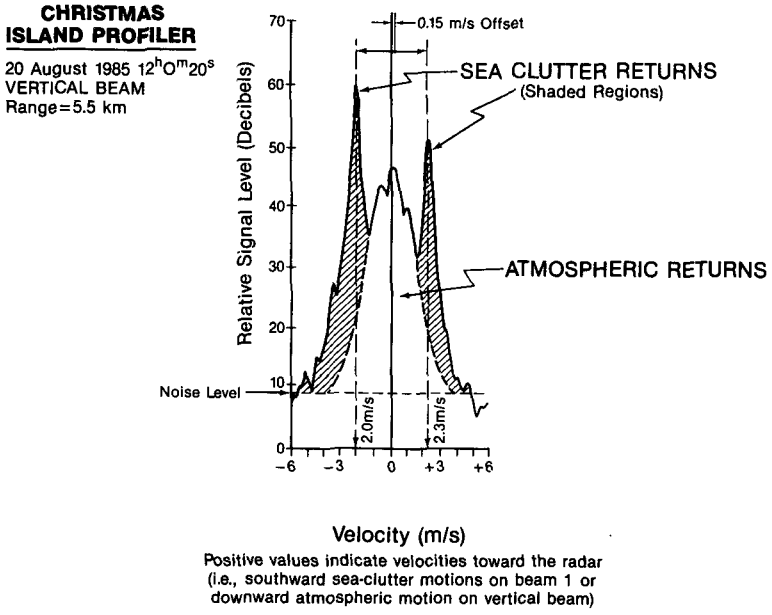

FIG. 2. Sample Doppler echo spectrum obtained on the vertical beam position at a range of 5.5 km, showing the normal atmospheric spectrum (unshaded) and the sea-scatter spectrum (shaded peaks) arising from sidelobe 1 shown in Fig. 1. Note that the sea-scatter peaks are separated by 4.3 m s^{-1} and that the offset of the mean value of this separation from zero indicates that the sea-surface current has a radial inward (i.e., toward the radar) drift of 0.15 m s^{-1}. See text for details.

area covered by the beams (in the following section, we will present arguments to support the homogeneity of the surface current at ranges greater than about 8 km from the coast). The surface current so derived is a measure of the mean Eulerian motion of the sea surface area in the region illuminated by the antenna beams. (Eulerian motion is that motion measured within a fixed spatial framework, in this case the ocean surface within the antenna beam.)

It is important to point out that the depth of the surface current measured by this radar method is frequency dependent (Broche et al., 1983) and, for a 50 MHz radar, is only about 25 cm.

Finally, although amplitude asymmetries of the two spectral peaks and additional second-order spectral characteristics may be used to infer surface wind magnitude and direction as well as sea state, these features will not be considered here.

3. Data presentation

Figure 3 shows a relatively continuous record of the components of V_d measured on beams 1 and 3 shown in Fig. 1, at ranges between 1.8 km and 12.6 km. The magnitude of each component is indicated on the respective ordinate. Blank periods correspond to periods when either the system was being tested or when our analysis algorithm determined that the sea-scatter echoes were much weaker than atmospheric echoes at the same range. A few additional periods (e.g., in the first four ranges near midday on 28 December) in Fig. 3, because of their irregular appearance, could possibly contain spurious velocities due to contamination from atmospheric echoes. Such contamination, however, consititutes only a small portion of the total record.

A major feature of the current components shown in Fig. 3 is the complexity of the patterns near the island, which gradually blends into a more homogeneous flow at increasing distances from the island. Moreover, the overall pattern of near-island currents appears to be dominated at different times by diurnal tides (e.g., 23–26 December), semidiurnal tides (e.g., 28–31 December), or a combination of both. The complex nature of the near-island results suggest that it would be impossible to deduce a mean direction of the currents, since homogeneity at comparable ranges on the two beams cannot be assumed.

Beyond about 8 km, however, the currents on both beam positions appear to be independent of range, except for a few instances that presumably arise from local surface current anomalies. Although we cannot be certain without further testing, we assume that the current components on all beam positions, beyond a range of about 7 km, are reasonably representative of open ocean currents. We support this assumption with four separate points: 1) the relatively constant nature of the current magnitude with increasing range, 2) the fact that ocean depth at these distances from the island is in excess of 1 km, so that island effects should be greatly attenuated, 3) the deduced mean flow toward the WNW is in a direction that would not be greatly affected by the presence of the island, and 4) the de-

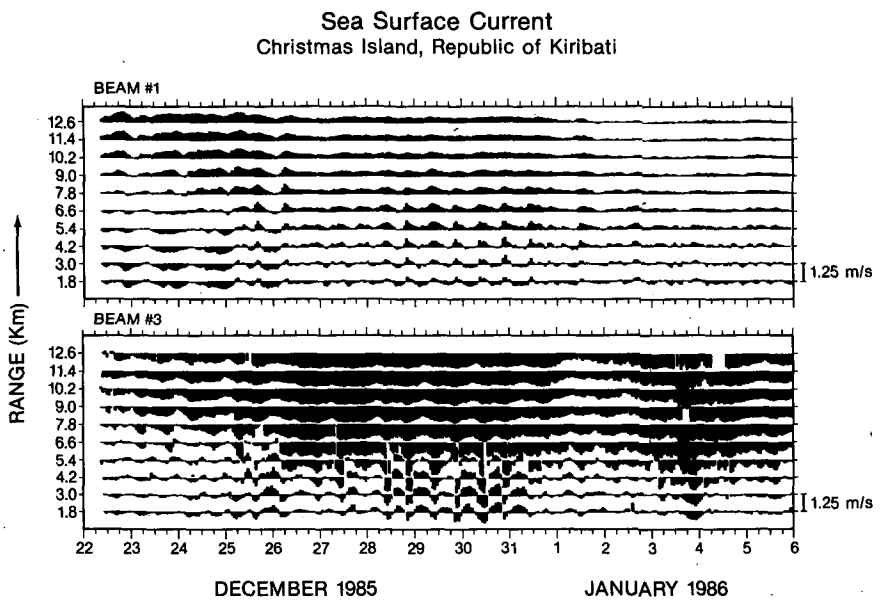

FIG. 3. Continuous 15-day record of the radial sea-surface current components on beams 1 and 3 as a function of range. Note the complex drift patterns between about 1.8 and 7.8 km, and the more coherent motion that can be seen at all ranges between 9.0 and 12.6 km. Values above/below the lines indicate radial velocities away from/toward the radar.

duced currents agree well with the currents discussed by Wyrtki et al. (1981) in the same general region of the Pacific.

A conventional "stick" plot of the sea surface current deduced from range-averaged values of V_d^k between 9 and 13.8 km on beams 1 and 3 is presented in Fig. 4a. Similar results using means 2 and 3, although not shown here, agree very well with the results in Fig. 4a. Results obtained using beams 1 and 2, on the other hand, exhibit some minor discrepancies relative to the other two plots. These discrepancies do not arise from inhomogeneities in the sea-surface current field, but rather from inherent measurement inaccuracies that arise from attempting to deduce an approximate westward current by using a pair of approximate northward current components having a small (15°) angular separation. Thus, in practice, full current vectors should be deduced only using antenna beam pairs having angular separations greater than, say, 30°.

It is important to point out that the overall conformity of the drifts, found by intercomparing results obtained using the two sets of beam pairs with the greatest angular separation, also attests to the homogeneity of the flow within the sampled area.

The average character of the surface currents presented in Fig. 4a suggests a mean motion toward the west-northwest at about 0.6 m s^{-1} throughout the three-month period of observation. It is also apparent, however, that the variability of the current magnitude is of the same order as the mean flow. Indeed, two brief periods can be seen centered on 26 November and 12 December, when the surface current essentially ceased. In addition, a relatively slow variation of the current magnitude, with a period of about 25 days, is apparent in Fig. 4a.

The vectorial presentation of the surface currents shown in Fig. 4a has been resolved into meridional and zonal components in Figs. 4b and 4c. While the same general character of both the mean flow and the slow variations are also apparent in this type of presentation, diurnal and semidiurnal tidal components become more obvious. These fluctuations are most apparent, for example, in the zonal (westward) flow between roughly 30 November and 31 December.

A power spectrum of both the zonal and meridional current fluctuation is shown in Fig. 5 for the period 23 November–27 February. Here we have included spectral periods between roughly 3 hours and 100 days. The increased length of the error bars with increasing period reflect the fact that the longer period portions of these spectra contain less spectral averaging than the shorter periods.

Preliminary examination of these spectra shows a number of interesting features. First, the (approximately) linear decrease of spectral power density with increasing frequency on this log–log plot fits a power law relationship with a $-\frac{3}{2}$ slope. Second, the zonal fluctuations appear to have roughly twice the spectral energy density as the meridional fluctuations at comparable periods. Third, diurnal and semidiurnal tidal fluctuations are clearly apparent on both spectra, with the zonal tidal fluctuations again containing roughly twice the energy density as the meridional fluctuations. Finally, we point to the presence of a significant peak

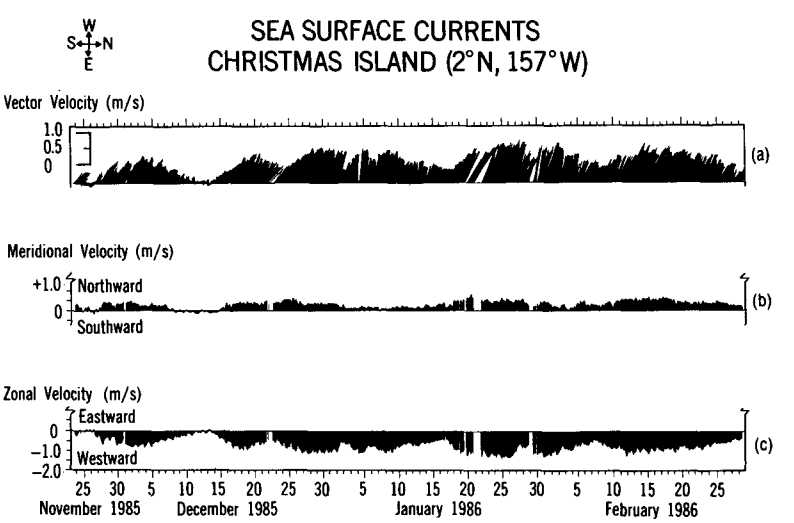

FIG. 4. (a) A conventional "stick" plot of the sea-surface current vector, spatially averaged over five ranges between 9.0 and 13.8 km, between 23 November 1985 and 27 February 1986. Magnitude appears on the left ordinate. The current direction is indicated by the small compass rose in the upper left corner. (b) and (c) show the meridional (north–south) and zonal (east–west) components of this current, which more clearly exhibit the diurnal and semidiurnal tidal features. Velocity scales and direction are indicated on the left of these figures.

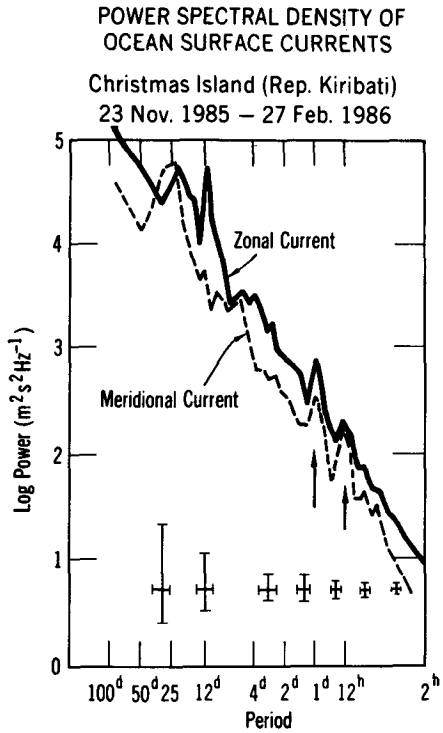

FIG. 5. Power spectra of the zonal and meridional current fluctuations between roughly 3 h and 100 days for the data shown in Fig. 4.

in the meridional spectrum at a period of about 25 days. That the peak is statistically significant is indicated by the 2 sigma (95% significance) error bars.

4. Discussion and conclusions

The results presented in the previous section outline a number of the general characteristics of sea surface currents in the central equatorial Pacific as observed by a VHF radar. These characteristics are itemized and discussed below.

1) Observed sea-surface current fluctuations near the island are quite complex and exhibit pronounced tidal fluctuations that vary greatly from day-to-day.

2) At sufficiently large distances from the island, the observed tidal fluctuations are greatly attenuated and the spectrum of current fluctuations appears to follow a $-3/2$ power law, at least for periods between 3 h and 100 days.

3) The spectral energy in the zonal fluctuation appears to be roughly twice as large as that in the meridional fluctuations. In addition, the spectra show a ~25-day periodicity that is most pronounced in the meridional component. This result is in agreement with earlier observations of 20–30 day surface waves in the equatorial Pacific reported in a number of studies (e.g., Legeckis, 1977; Wyrtki, 1978; Weisberg et al., 1979; Wyrtki et al., 1981; Legeckis et al., 1983; Hansen and Paul, 1984; and Philander et al., 1985). Indeed, Philander (1978) has shown that westward-propagating waves with wavelengths of about 1000 km and periods of about one month can be generated just north of the equator on the edges of the narrow South Equatorial Current.

4) At a sufficient distance from the shore the ~0.6 m s^{-1} average (Eulerian) current of the sea surface toward the west-northwest compares favorably with earlier current meter measurements by Wyrtki et al. (1981) at 153°W during the January 1980, and with the average zonal surface current profile shown in Philander (1978).

The idea of using VHF radars to monitor sea surface currents is clearly not new. Except for a few significant differences in the technique described above, the method has been well demonstrated by previous studies. Nevertheless, there are two unique aspects of our study that need to be stressed here.

First, our results represent the first continuous sea-surface current measurements made by radar in the tropical Pacific, and, as such, demonstrate the potential of monitoring both the mean and the fluctuating components of sea surface currents on a long-term continuous basis at remote locations. We feel this to be a major point, since the tropical Pacific is a region being actively studied in the context of its impact on worldwide climate variability. Moreover, Christmas Island at 2°N lies well within the "equatorial waveguide" (e.g., Gill, 1982), a region delineated by a narrow belt of latitudes that can contain a infinite set of equatorially trapped waves. Thus, continuous surface current data from Christmas Island (or similar sites) would provide a valuable addition to existing monitoring programs for the mean drift, as well as its short- and long-term variability.

Second, the results reported here were obtained at an existing wind profiler field site with an existing analysis system and only minimal radiated power (~1 watt average). Subsequent to these observations the profiler antenna was modified to eliminate sea-scatter returns, so that ongoing measurements using the existing system are not possible. It is not unreasonable to expect, however, based upon the above results, that relatively inexpensive additions to established Pacific profiler sites could be made to establish continuous sea-surface drift measurements for the next few years. Such data, when coupled with concurrent surface winds and winds aloft data from the same locations, would provide unique yet inexpensive supplemental data bases to study ocean–atmosphere interactions, as well.

Acknowledgments. We are happy to acknowledge useful discussions with J. McWilliams and W. Large of the National Center for Atmospheric Research, D. Hansen of NOAA's Atlantic Oceanographic and Meteorological Laboratory, R. Woodman of the Instituto

Geofísico del Peru, and T. Barnett of the Scripps Institute for Oceanography. P. Broche and M. Crochet of the Laboratories de Sondages Electromagnnétiques de Environment Terrestre (LSEET), Université de Toulon, France, provided valuable insights into various aspects of radar sea scattering.

REFERENCES

Barrick, D. E., 1972: First-order theory and analysis of MF/HF/VHF scatter from the sea. *IEE Trans. Antennas and Propag.*, **AP-20,** 2–10.

——, J. M. Headrick, R. W. Bogle and D. C. Crombie, 1974: Sea backscatter at HF: Interpretation and utilization of the echo. *Proc. IEEE,* **62,** 673–680.

Broche, P., J. C. Maistre and P. Forget, 1983: Measure par radar décamétrique cohérent des courants superficiels engendrés par le vent. *Oceanol. Acta,* **6,** 43–53.

——, P. Forget, J. C de Maistre, J. L. Devenon and M. Crochet, 1987: VHF radar for ocean surface current remote-sensing. Submitted to *J. Atmos. Oceanic Technol.*

Ecklund, W. L., D. A. Carter and B. B. Balsley, 1979: Continuous measurement of upper atmospheric winds and turbulence using a VHF Doppler radar: Preliminary results. *J. Atmos. Terr. Phys.,* **41,** 983–994.

Gill, A. E., 1982: *Atmosphere–Ocean Dynamics, Vol. 30.* Academic Press.

Hansen, D. V., and C. A. Paul, 1984: Genesis and effects of long waves in the Equatorial Pacific. *J. Geophys. Res.,* **89**(C6), 10,431–10,440.

Legeckis, R., 1977: Long waves in the eastern equatorial Pacific Ocean: A view from a geostationary satellite. *Science,* **197,** 1179–1181.

——, W. Pichel and G. Nesterczuk, 1983: Equatorial long waves in geostationary satellite observations and in a multichannel sea surface temperature analysis. *Bull. Amer. Meteor. Soc.,* **64,** 133–139.

Lipa, B. J., and D. E. Barrick, 1982: Analysis methods for narrow-beam high-frequency radar sea echo. NOAA Tech. Rep. ERL 420-WPL 56.

——, and ——, 1986: Extraction of sea state from HF radar sea echo: Mathematical theory and modeling. *Radio Sci.,* **21,** 81–100.

Philander, S. G. H., 1978: Instabilities of zonal equatorial currents, 2. *J. Geophys. Res.,* **83**(C7), 3679–3682.

Philander, G., D. Halpern, D. Hansen, R. Legeckis, L. Miller, C. Paul, R. Watts, R. Weisberg and M. Wimbush, 1985: Long waves in the equatorial Pacific Ocean, *Eos,* **66**(14), 154–156.

Weisberg, R. H., A. Horigan and C. Colin, 1979: Equatorially trapped Rossby–gravity wave propagation in the Gulf of Guinea. *J. Mar. Res.,* **37,** 67–86.

Wyrtki, K., 1978: Lateral oscillations of the Pacific Equatorial countercurrent. *J. Phys. Oceanogr.,* **8,** 530–532.

——, E. Firing, D. Halpern, R. Knox, G. J. McNally, W. C. Patzert, E. D. Stroup, B. A. Taft and R. Williams, 1981: The Hawaii to Tahiti shuttle experiment. *Science,* **211,** 22–28.